Available online at www.sciencedirect.com
ScienceDirect
International Journal of Thermal Sciences 48 (2009) 626–644
International Journal of Thermal Sciences
www.elsevier.com/locate/ijts

Coabsorbent cycles. Part one: Theory

Mihail-Dan N. Staicovici *

S.C. Varia Energia S.R.L. & S.C. Incorporate Power-Absorption Engineering S.R.L., str. Mihail Eminescu, nr. 81 B, floor 4, apart. 9, sector 2, 020 072 Bucuresti, Romania

Received 2 January 2007; received in revised form 6 May 2008; accepted 14 May 2008

Available online 18 June 2008

Abstract

Theoretical research laying down the basis of coabsorbent technology is presented. A coabsorbent cycle is built up by joining resorption cycle subcycles along a common isostere ($y = y_M = \text{const.}$), so that opposed pair processes, of generation and resorption, and of absorption and desorption, are isobar or non-isobar and in mass (vapour) and heat exchange, and subcycles separate absorbents have a common point "M" (mixing point), where they are mixing up and cyclic regenerate the absorbent of mean concentration, y_M. Paper includes nontruncated and truncated coabsorbent cycles, truncation theory, fractals, columns, COP estimate, new cycles with pressure and concentration stages, advanced cycles transposition into coabsorbent technology and model results for each. Coabsorbent cycle application could bring practical and efficiency increase advantages in absorption technology by: a) elimination of vapour rectification need; b) elimination of absorbent inventory problem; c) increase of cycle match with gliding sources and source-task; d) noncondensable refrigerant operation capacity; e) favouring behaviour for control and optimization; f) gax effect use and cycle exergy efficiency increase favouring; g) cycle complexity decrease; h) capacity to transpose known condensation absorption cycles, and create new useful ones.

Keywords: Thermal absorption; Cooling and heating nontruncated coabsorbent cycles; Coabsorbent cycle truncation; Cooling and heating fractals; Advanced (multi-effect) coabsorbent cycles

1. Introduction

The coabsorbent cycles have been publicly disclosed in the two last years by their author in published works on heat pumping and power applications [1–16]. In this paper, theoretical research laying down the basis of coabsorbent cycles technology are presented, including nontruncated and truncated coabsorbent cycles, theory of truncation, cooling and heating fractals, truncation columns, column cycles, coabsorbent cycles COP estimate, new cycles with pressure and concentration stages and multi-effect cycles transposition into coabsorbent technology.

2. Nontruncated heating and cooling coabsorbent cycles

For the sake of completeness, the main ideas of the coabsorbent cycles are remembered first. So far, the absorbent administration in an absorption cycle, including two or more subcycles (interconnected by mass and/or heat transfer), bases on a common, known practice that, in short, could be expressed by "a separate absorbent flow in each individual subcycle". In a previous work [1], the author is proposing a new type of absorption cycles, with a different absorbent administration, and named "with co-absorbent", or simpler, *coabsorbent cycles*. In this way, using coabsorbent cycles all condensation and resorption cycle problems (e.g. reduced solubility field, rectification need, absorbent migration, or cycle complexity increase with COP improvement) can be avoided. The key of coabsorbent cycles are the resorption ones [17]. Relative recent works concerning resorption cycles have been accomplished for cooling with water/lithium bromide [18], or for evaluation of absorption and resorption heat pumps COP with ammonia–water as working fluids [19]. The coabsorbent cycle is built up by joining the resorption cycle subcycles along a common isostere ($y = y_M = \text{const.}$), so that the opposed pair isobar or non-isobar processes, of generation and resorption, and of absorption and desorption, are in mass (vapour) and heat exchange, and the subcycles separate absorbents have a common point "M" (mix-

* Tel.: +4021 210 65 00; +40720 26 25 89.
E-mail addresses: mihail_dan_staicovici@yahoo.com, staicovici@upcmail.ro, staicovici@dnt.ro.

1290-0729/$ – see front matter
doi:10.1016/j.ijthermalsci.2008.05.004

Nomenclature

a	absorption absorbent inlet flow	kg/kg
a_1	absorption absorbent outlet flow	kg/kg
COP	coefficient of performance	
d	desorption absorbent inlet flow	kg/kg
d_1	desorption absorbent outlet flow	kg/kg
f	cumulated absorbent flow	kg/kg
g	generation absorbent inlet flow	kg/kg
g_1	generation absorbent outlet flow	kg/kg
h	truncated column height	K^{-1}
i	liquid absorbent specific enthalpy	J/kg
I	vapour absorbent specific enthalpy	J/kg
p	pressure	N/m^2
q	heat	J
r	resorption absorbent inlet flow	kg/kg
r_1	resorption absorbent outlet flow	kg/kg
S	coabsorbent cycle symmetry factor	
T	temperature	K
V	vapour mass	kg
w	mechanical work	J
y	liquid absorbent mass concentration	kg/kg
Y	vapour mass concentration	kg/kg

Greek

Δ	difference
η	effectiveness

Subscripts

A	absorption
acc	advanced cooling cycle
D	desorption
c	compressor, cooling
cf	cooling fractal
coabs	coabsorbent
C	Carnot
gax	generation absorption heat exchange
G	generation
i, j, k	current index
I	inlet
h	heating
hf	heating fractal
M	mixing
opt	optimal
O	outlet
psccac	pressure stage coabsorbent cooling advanced cycle
R	resorption
t	truncated
nt	nontruncated
u	unitary
w	referring to cycle work input

ing point), where they are mixing up and cyclic regenerate the absorbent of mean concentration, y_M. By joining upon temperature decrease two cooling + heating type subcycles, it is obtained a *nontruncated cooling coabsorbent cycle*, Fig. 1, and by joining upon temperature decrease two heating + cooling type subcycles, it is obtained a *nontruncated heating* (*heat transformer*) *coabsorbent cycle*, Fig. 4 [1]. The coabsorbent cycles are new, individual thermodynamic absorption ones, with different flow and heat properties as compared to condensing cycles (with separate absorbent flow). Because of theirs intrinsic features, they can operate as independent, or as satellite cycles, recovering heat from other main cycles, as they are place independent (can be placed to work anywhere in the working combination solubility field, as being adapted to any sources supply). First, we shall deal with nontruncated cycles, which have great theoretical importance. Second, we shall introduce the truncated coabsorbent cycles, which have great practical importance.

2.1. Nontruncated cooling coabsorbent cycle

The nontruncated coabsorbent cooling cycle is plotted in a $\log p - 1/T$ diagram, Fig. 1(a). Its operation is as follows (see arrows): absorbents exiting low pressure desorber and absorber are being mixed up in M, the resulting cumulated flow f_M leaves mixer with concentration y_M and then is pumped and distributed in pre-established complementary quantities to the high pressure generator and resorber, and finally, absorbents exiting resorber and generator are expanded to the low pressure desorber and absorber, in order to close the cycle. Cooling cycle input data are resorber outlet temperature (sink source related) and concentration, T_{RO} and y_{RO}, respectively, desorber inlet temperature (related to useful cooling effect lowest temperature), T_{DI}, and generator outlet temperature (heat source related), T_{GO}. From these four parameters it results the rest of the other parameters: p_{AD}, p_{GR}, T_M $(= T_{RO})$, y_M, and y_{GO}. We define the following specific inlet and outlet mass flow factors (kg absorbent/kg refrigerant) for absorber, generator, resorber, and desorber, Table 1. Vapour concentration must be higher than a certain minimum value, the (*vapour*) *threshold concentration*. Cooling cycle has the y_{RO} value as threshold concentration, that is for $r > 0$ we must have $Y_G > y_{RO}$ in order that resorber be capable to reach its y_{RO} designed outlet concentration (see Eq. (3)). Having problems with threshold concentration means that this condition cannot be fulfilled. Cycle parameters are expressed in equations given in Table 2. Devices partial mass balance result in Eqs. (9) and (10), where V_{GD} is the ratio of the vapour generated by generator, V_G, through that of desorber, V_D (chosen at random, $V_D = 1$ here), Eq. (11). From the division of Eqs. (9) and (10), term by term, we obtain the *typical nontruncated cooling coabsorbent cycle equation*, Eq. (12). This shows the relation between cycle unknown (a and d) and known (g_1 and r_1) specific flow factors and concentrations y_{RO}, y_{GO} and y_M. Also, it defines cycle S *symmetry factor* (see last ratio in Eq. (12)), revealing how much flow factors and specific heat of each adjacent opposite processes (generation/resorption,

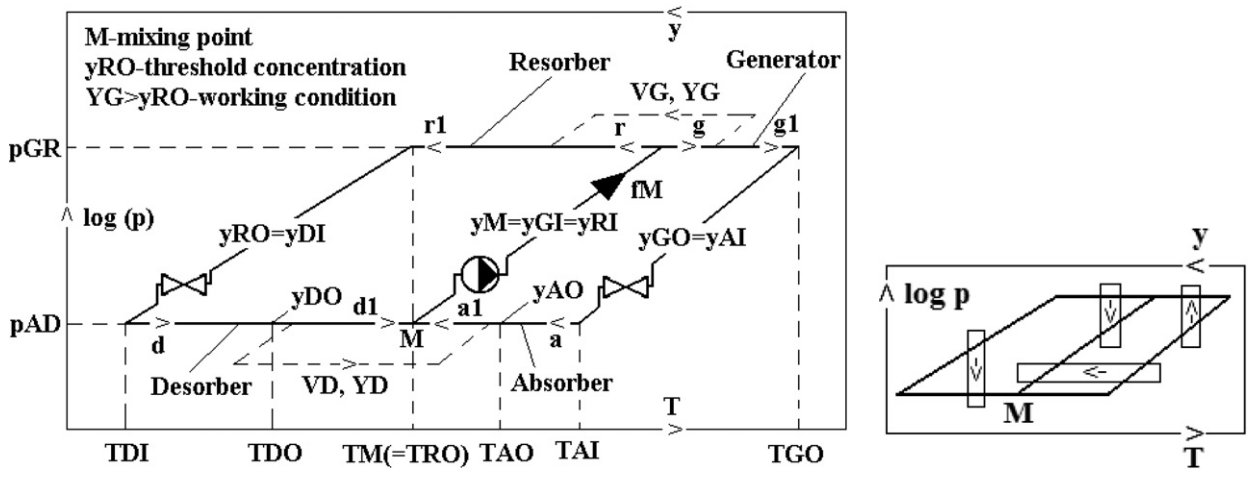

(a) (b)

Fig. 1. The nontruncated cooling coabsorbent cycle.

Table 1
Inlet and outlet absorber, generator, resorber, and desorber mass flow factors

Device	Absorber		Generator		Resorber		Desorber	
Inlet	$a = \frac{Y_D - y_{AO}}{y_{AO} - y_{AI}}$	(1)	$g = \frac{Y_G - y_{GO}}{y_{GI} - y_{GO}}$	(2)	$r = \frac{Y_G - y_{RO}}{y_{RO} - y_{RI}}$	(3)	$d = \frac{Y_D - y_{DO}}{y_{DI} - y_{DO}}$	(4)
Outlet	$a_1 = a + 1 = \frac{Y_D - y_{AI}}{y_{AO} - y_{AI}}$	(5)	$g_1 = g - 1 = \frac{Y_G - y_{GI}}{y_{GI} - y_{GO}}$	(6)	$r_1 = r + 1 = \frac{Y_G - y_{RI}}{y_{RO} - y_{RI}}$	(7)	$d_1 = d - 1 = \frac{Y_D - y_{DI}}{y_{DI} - y_{DO}}$	(8)

Table 2
Most important nontruncated cycle parameters

Cycle	Cooling nontruncated		Heating nontruncated	
Devices partial mass balance	$V_{GD} r_1 = d$	(9)	$V_{DG} a_1 = g$	(19)
	$V_{GD} g_1 = a$	(10)	$V_{DG} d_1 = r$	(20)
	$V_{GD} = \frac{V_G}{V_D}$	(11)	$V_{DG} = \frac{V_D}{V_G}$	(21)
Typical equation	$\frac{a}{d} = \frac{g_1}{r_1} = S = \frac{y_{RO} - y_M}{y_M - y_{GO}} = \text{const.} > 0$	(12)	$\frac{g}{r} = \frac{a_1}{d_1} = S = \frac{y_M - y_{DO}}{y_{AO} - y_M} = \text{const.} > 0$	(22)
Cycle mass balance	$f_M = V_{GD}(g_1 + r_1) = a_1 + d_1$	(13)	$f_M = V_{DG}(a_1 + d_1) = r_1 + g_1$	(23)
Derived equations	$\frac{V_{GD} g_1}{f_M} = \frac{a}{f_M} = \frac{S}{S+1}$	(14)	$\frac{V_{DG} a_1}{f_M} = \frac{g}{f_M} = \frac{S}{S+1}$	(24)
	$\frac{V_{GD} r_1}{f_M} = \frac{d}{f_M} = \frac{1}{S+1}$	(15)	$\frac{V_{DG} d_1}{f_M} = \frac{r}{f_M} = \frac{1}{S+1}$	(25)
Mixing concentrations	$y_{DO} = y_{DI} - \frac{Y_D - y_{DI}}{r_1 V_{GD} - 1}$	(16)	$y_{GO} = y_{GI} - \frac{Y_G - y_{GI}}{a_1 V_{DG} - 1}$	(26)
	$y_{AO} = y_{AI} + \frac{Y_D - y_{AI}}{g_1 V_{GD} + 1}$	(17)	$y_{RO} = y_{RI} + \frac{Y_G - y_{RI}}{d_1 V_{DG} + 1}$	(27)
Mixer mass balance	$d_1 y_{DO} + a_1 y_{AO} = (d_1 + a_1) y_M$	(18)	$r_1 y_{RO} + g_1 y_{GO} = (r_1 + g_1) y_M$	(28)

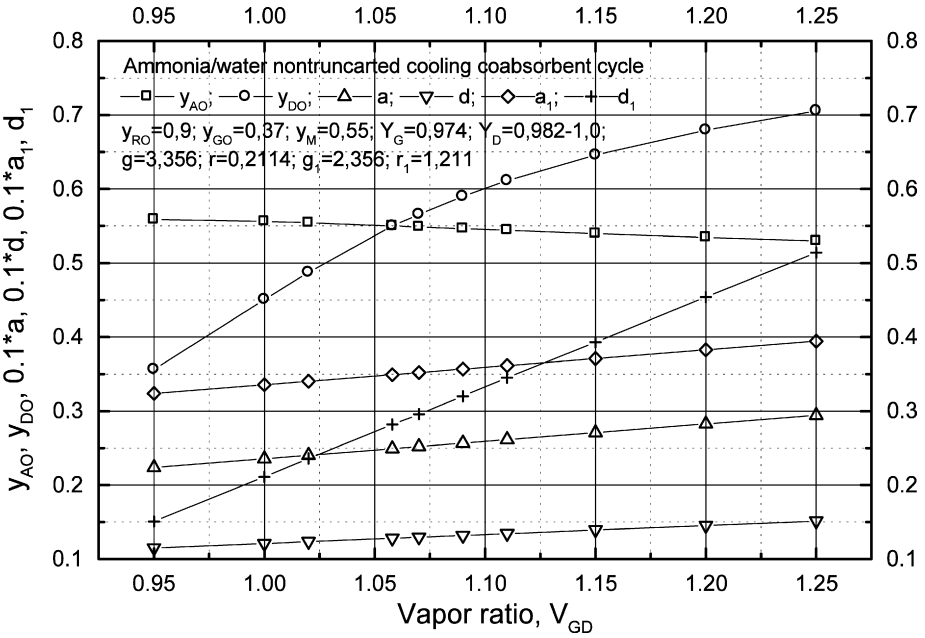

Fig. 2. Flow analysis case study of a nontruncated cooling coabsorbent cycle.

absorption/desorption) are different. Close to unity S values indicate cycle design good symmetry with respect to y_M isostere and relative small differences between flows and specific heats, while its far from unity values indicate the contrary. The simple mass balance on the cycle results also in Eq. (13), wherefrom, with Eq. (12) we obtain Eqs. (14) and (15). Cycle a and d flow factors depend on desorber and absorber end mixing concentrations, y_{DO} and y_{AO}, respectively, which can be determined directly, if $Y_D = 1$ (nonvolatile absorbent case), or after an iterative process, if $Y_D < 1$ (volatile absorbent case), from Eqs. (1), (4), (9) and (10), resulting in Eqs. (16) and (17), respectively. In practice, we choose a value for V_{GD} and calculate y_{DO} and y_{AO} so that they have desired values usually in the range of $y_M \leqslant y_{DO} \leqslant y_{DI}$, and $y_M \geqslant y_{AO} \geqslant y_{AI}$, respectively, that is desorber and absober processes end temperatures are smaller than the mixer temperature, $T_{DO} \leqslant T_M$ and higher than that, $T_{AO} \geqslant T_M$, respectively. This situation would characterize a normal cycle operation. However, if this were not true, that is accidentally or systematically we have $T_{DO} \geqslant T_M$ and $T_{AO} \leqslant T_M$, respectively, when sources favour cycle COP increase, then desorber outlet concentration y_{DO} decreases below mixing point concentration, $y_M \geqslant y_{DO}$ and absorber outlet concentration y_{AO} exceeds it, $y_M \leqslant y_{AO}$, but in all cases Eqs. (16) and (17) verify unconditionally mass balance on mixer M, which for refrigerant is written as Eq. (18). In other words, mixing concentration y_M is achievable with mixing absorbents having alternatively end concentration below and above the y_M, around the *balance point*, which is characterizing cycle operation with desorber and absorber end concentrations equal to that of the mean concentration, $y_{DO} = y_{AO} = y_M$. The balance point corresponds to V_{GD} ratio equal to unity, in case of pure refrigerant, only, that is $Y_D = 1$. In Fig. 2 we present results of an ammonia/water case study [1], showing features described above. Here we considered resorber and generator outlet concentrations as $y_{RO} = 0.9$ and $y_{GO} = 0.37$, respectively, and mean concentration $y_M = 0.55$. Mean generator vapour concentration is $Y_G = 0.974$ and that of desorber was variable, $Y_D = 0.982 - 1.0$. Pressure and temperature data in the cycle main points are: $p_{GR} = 11$ bar, $p_{AD} = 5$ bar, $T_{GO} = 90\,^{\circ}\text{C}$, $T_{GI} = T_{RI} = 55\,^{\circ}\text{C}$, $T_{RO} = T_M = 30\,^{\circ}\text{C}$, $T_{DI} = 7\,^{\circ}\text{C}$, $T_{AI} = 60\,^{\circ}\text{C}$. Concentration threshold condition is fulfilled because $Y_G > y_{RO}$. Applying Eqs. (2) and (3), generator and resorber inlet flow factors resulted in $g = 3.356$ and $r = 0.2114$. Outlet generator and resorber flow factors resulted applying Eqs. (6) and (7), respectively, $g_1 = 2.356$ and $r_1 = 1.2114$. Balance point $y_{DO} = y_{AO} = y_M = 0.55$ is reached when vapour ratio is $V_{GD} \cong 1.06$, different from unity, because $Y_D \leqslant 1$. Mixer mean concentration can be achieved alternatively, whether with absorbent flows a_1 of concentrations $y_{AO} < y_M = 0.55$ and temperatures $T_{AO} > T_M = 30\,^{\circ}\text{C}$ mixed up with absorbents d_1 of concentrations $y_{DO} > y_M = 0.55$ and temperatures. $T_{DO} < T_M = 30\,^{\circ}\text{C}$ if cycle worked in the right side of the balance point where $V_{GD} > 1.06$ and normal cycle operation is met, or with absorbent flows a_1 of concentrations $y_{AO} > y_M = 0.55$ and temperatures $T_{AO} < T_M = 30\,^{\circ}\text{C}$ mixed up with absorbents d_1 of concentrations $y_{DO} < y_M = 0.55$ and temperatures $T_{DO} > T_M = 30\,^{\circ}\text{C}$ if cycle worked in the left side of the balance point where $V_{GD} < 1.06$ and sources temperatures favour cycle COP increase. Absorbent exits desorber and absorber with temperatures varying within $T_{DO} = (63\text{–}16)\,^{\circ}\text{C}$ and $T_{AO} = (28.5\text{–}32.5)\,^{\circ}\text{C}$, respectively, when vapour ratio V_{GD} covers the abscissa in Fig. 2, $V_{GD} = 0.95\text{–}1.25$. As prior mentioned, balance point left side is a higher cooling COP region as compared to the right one. Indeed, here cycle works on broader desorption and absorption temperature intervals, with comparatively higher and lower mean values, respectively, which according to Lorentz absorption cooling COP favours efficiency increase. Fig. 2 plots as well desorber and absorber

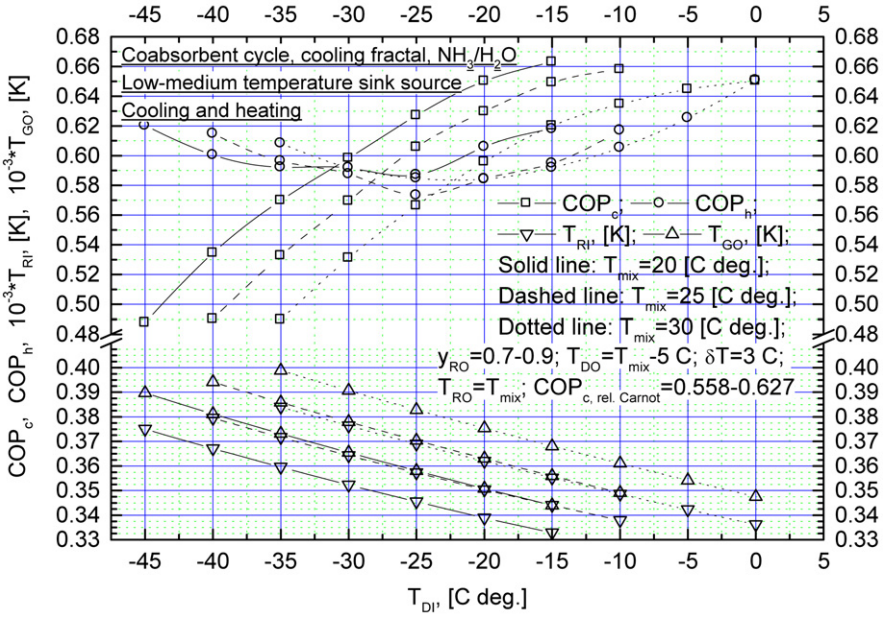

(a)

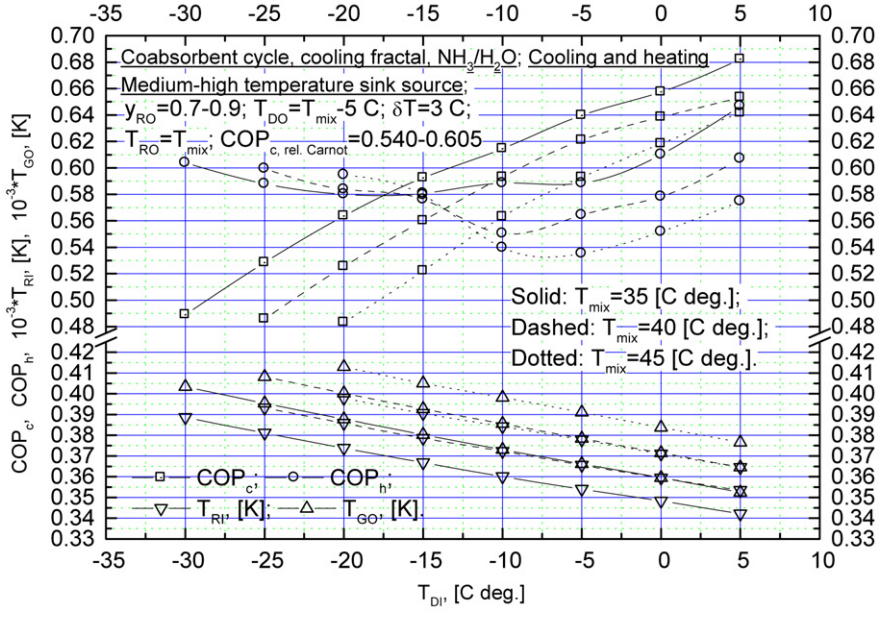

(b)

Fig. 3. Coabsorbent cooling nontruncated cycle COP_c, co-generated heating effect COP_h, generator outlet temperature, T_{GO}, and resorber inlet temperature, T_{RI}, against desorber inlet temperature, T_{DI}, for low-medium and medium-high sink temperatures, $T_{mix} = T_M$, (a) and (b), respectively.

flow factors for this case study, which decrease linearly with decreasing vapour ratio.

Cooling cycle COP_c, equal to (desorber heat input/generator heat input), has been modeled and comments follow. Nontruncated cooling cycle has interesting thermal features, Figs. 3(a), (b): (i) good efficiency relative to Carnot, $COP_{c,rel.Carnot} =$ 0.558–0.627 and $COP_{c,rel.Carnot} =$ 0.540–0.605, in cases (a) and (b), respectively; (ii) industrial cooling (−40 to −45 °C), is about 1.5 times higher then condensing cycle COP [17]; (iii) air conditioning COP approaches that of H_2O/LiBr system; (iv) unlike condensing cycle, the nontruncated cooling one works in cogeneration of cooling and heating (through the additional heat delivered by its resorber), $COP_h =$ resorber heat output/generator heat input.

2.2. *Nontruncated heating (heat transformer) coabsorbent cycle*

The nontruncated heating coabsorbent cycle is plotted in the $\log p - 1/T$ diagram in Fig. 4. It is contrary covered by the absorbent flow as compared to the cooling cycle in Fig. 1 and formally it can be obtained rotating the cooling cycle by 180 degrees in the plot diagram plane. A flow chart including some features of the nontruncated heating coabsorbent cycle has been

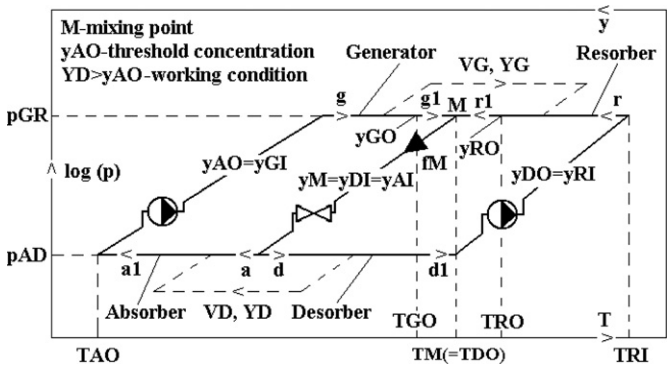

Fig. 4. The nontruncated heating (heat transformer) coabsorbent cycle.

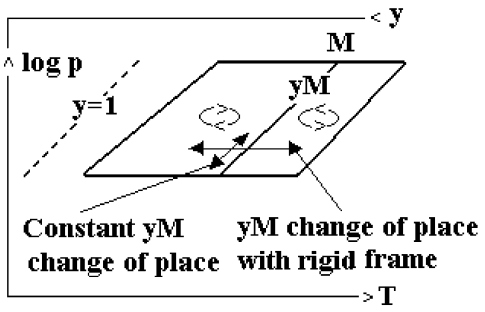

Fig. 5. Coabsorbent cycle change of place.

proposed in a "Self Regenerated Absorption Temperature Amplifier" (SRATA) by [20], but author neither considered SRATA as a coabsorbent cycle, nor had foresaw advantages of this more general class of absorption cycles, having condensing absorption as a particular case. Its operation is as follows (see arrows): the absorbents exiting the high pressure resorber and generator are being mixed up in M, the resulting cumulated flow f_M leaves the mixer with concentration y_M and then is expanded and distributed in pre-established complementary quantities to the low pressure absorber and desorber, and finally, the absorbents exiting the desorber and the absorber are pumped to the high pressure resorber and generator, in order to close the cycle. Heating coabsorbent cycle has input data, desorber outlet temperature (heat source related) and concentration, T_{DO} and y_{DO}, respectively, resorber inlet temperature (related to useful heating effect maximum temperature), T_{RI}, and absorber outlet temperature (sink source related), T_{AO}. From these four parameters it results the rest of useful parameters: p_{AD}, p_{GR}, T_M $(= T_{DO})$, y_M, and y_{AO}. Flow factors, defined in Eqs. (1)–(8), hold true also. The threshold concentration is here y_{AO}, that is for operation we must have $Y_D > y_{AO}$. Most important parameters are given in Table 2. As compared to the classic condensing heat transformer, which has $y_{AO} = y_{GI} \cong 1.0$, the coabsorbent cycle operates with a smaller temperature lift, equal to $(T_{RI} - T_{DO})$, and a smaller absorber end temperature T_{AO}, for same generation end temperature T_M $(= T_{DO})$. Similarly to the condensing cycle, temperature lift increase is requiring absorber cooling till temperatures T_{AO} which sink sources not always can supply.

2.3. Cycle change of place

During operation, cycle-sources interaction may change. Two particular changes of place can happen when $f_M = \text{const.}$, schematically shown in Fig. 5. First cycle changing the place is up and down along the mean concentration isostere, keeping it constant. During this operation, cycle extreme isosteres value may change. The second, could happen when keeping constant the extreme isosteres and pressures (rigid frame) and changing y_M value. Next we shall give simple equations of both cases, for cycles analyzed, included in Table 3. For the cooling cycle, from Eq. (12) written as Eq. (29), and Eq. (30), we obtain the flow factors with $y_M = \text{const.}$ change of place given by Eqs. (31) and (32). In this case, cycle frame (concentrations y_{RO} and y_{GO} and corresponding pressure stages) may undergo modifications, which alter a and d values, but keep $y_M = \text{const.}$ The y_M change of place with rigid frame operation is obtained from Eqs. (31) and (32), as Eqs. (33) and (34). As we remark, y_M depends linearly by a or d. This behaviour could be useful in cycle control and optimization. Concerning heating cycle, we consider Eq. (22) written as Eq. (35), and Eq. (36), wherefrom, when $y_M = \text{const.}$, flow factors are given by Eqs. (37) and (38). Similarly, cycle frame (concentrations y_{AO} and y_{DO}) may undergo modifications, which alter g and r values, but keep $y_M = \text{const.}$ The y_M change of place with rigid frame operation is obtained from Eqs. (37) and (38), as Eqs. (39) and (40), which keep same linear expression with respect to g or r flow factors.

2.4. Nontruncated coabsorbent-condensing cycle

Nontruncated cooling and heating cycles work only if $Y_G > y_{RO}$ and $Y_D > y_{AO}$, respectively. When $Y_G = y_{RO}$ and $Y_D = y_{AO}$, resorption and absorption processes, respectively, are replaced each by condensing processes and cycles become nontruncated cooling and heating condensing-coabsorbent cycles, Figs. 6(a), and (b), respectively. Resorption and absorption processes vanish, so are represented by dotted lines, but opposed isobar processes finish by mixing absorbents in mixer, and are represented by solid line. Such cycle is met for instance in single-stage NH_3/H_2O operation with incomplete or without vapour rectification. Cooling effect is produced on a broader desorption interval and resulting absorbent is mixed up with the absorbent exiting from absorber, prior to enter the recovering heat exchanger and generator. For this particular cycle, Eqs. (3) and (1) take this time values $r = 0$, and $a = 0$, respectively. When $Y_G = y_{RO} = 1.0$, or $Y_D = y_{AO} = 1.0$, cycles become simple condensing cycles (e.g. H_2O/LiBr).

2.5. Non-isobar nontruncated coabsorbent cycles

The isobar nontruncated cycles are particular cases of *non-isobar nontruncated coabsorbent cycles*, which join again resorption cycle subcycles along a common isostere ($y = y_M = \text{const.}$) and subcycles separate absorbents have as well a common point "M" (mixing point), cyclic regenerating the absorbent mean concentration, y_M, but opposed pair processes, of generation–resorption and absorption–desorption, are non-

Table 3
Change of place in nontruncated cycles

Cycle	Cooling nontruncated		Heating nontruncated	
Change of place at $y_M = \text{const.}$	$\frac{a}{d} = S$	(29)	$\frac{g}{r} = S$	(35)
	$(a+d)V_D = f_M = \text{const.}$	(30)	$(r+g)V_G = f_M = \text{const.}$	(36)
	$a = \frac{f_M}{V_D}\frac{y_{RO} - y_M}{y_{RO} - y_{GO}}$	(31)	$g = \frac{f_M}{V_G}\frac{y_M - y_{DO}}{y_{AO} - y_{DO}}$	(37)
	$d = \frac{f_M}{V_D}\frac{y_M - y_{GO}}{y_{RO} - y_{GO}}$	(32)	$r = \frac{f_M}{V_G}\frac{y_{AO} - y_M}{y_{AO} - y_{DO}}$	(38)
Change of place with rigid frame	$y_M = y_{RO} - \frac{a}{f_M/V_D}(y_{RO} - y_{GO})$	(33)	$y_M = y_{DO} + \frac{g}{f_M/V_G}(y_{AO} - y_{DO})$	(39)
	$y_M = y_{GO} + \frac{d}{f_M/V_D}(y_{RO} - y_{GO})$	(34)	$y_M = y_{AO} - \frac{r}{f_M/V_G}(y_{AO} - y_{DO})$	(40)

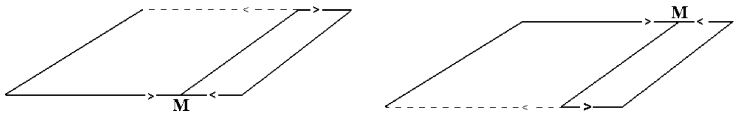

(a) (b)

Fig. 6. The nontruncated cooling (a), and heating (heat transformer) (b) coabsorbent-condensing cycles, plotted in the $\log p - 1/T$ diagram.

isobar and in mass (vapour) and heat exchange. Resulting cycles are in this case hybrid, exchanging not only heat with the sources, but also mechanical work (they use besides pure absorption processes, mechanical vapour compression too, or produce mechanical power). Most interesting of them are given in Fig. 7. Theoretical considerations outlined in Sections 2.1–2.4 apply here as well. These cycles have great application in practice, some being patent filled by the author (e.g. trigeneration cycles applied in rural areas, with global efficiency 1.12–1.5 and exergy efficiency 0.7–0.8, hybrid heat pump, cogeneration, etc. [12,13]).

3. A few new coabsorbent cycle configurations

Coabsorbent cycles number is huge. Their selection with criteria such thermodynamics principles respect and low complexity, usefulness and feasibility accomplishment, is mandatory. We show here the simplest, with potential applications, derived through nontruncated cycles composition, as: a) internal; b) external, and c) joined (skipped here). We start with the internal one, the truncation.

3.1. Internal composition – coabsorbent cycle truncation

Truncation is an important and unique technique of the coabsorbent technology. It enables nontruncated coabsorbent cycles to work either with smaller temperature heat sources for generation and desorption processes and same sink source temperature, in case of the cooling operation, $T_{GO} \leqslant T_{GO,\text{nt}}$, Fig. 8(a), or with higher temperature sink sources for absorption and resorption processes and same heat source temperature, $T_{AO} \geqslant T_{AO,\text{nt}}$, in case of the heating (heat transformer) operation, Fig. 8(b). Truncation is done upon a certain *heat* (*source*) *truncation line*, marking the end temperature of the generation and desorption processes in case of the cooling cycles, Fig. 8(a), and upon a *sink* (*source*) *truncation line*, marking the end temperature of the absorption and resorption processes in case of the heating cycles, Fig. 8(b). Truncation lines can be designed in a free or in a pre-established way, according to sources characteristics, Fig. 8. Both cooling and heating nontruncated coabsorbent cycles have same time desorption–generation and absorption–resorption processes, therefore can benefit of a double truncation. The two truncation lines define a *truncation column*, intrinsically related to a truncated cycle and referred to later in this paper. Most applications have quasi-constant temperature heat and sink sources, equal within the accuracy limits of the necessary heat exchange temperature pinch to mixing points temperatures, $T_{GO} = T_{M_{\text{heating}}} = \text{const.}$, e.g. (40–70) °C, and $T_{RO} = T_{M_{\text{cooling}}} = \text{const.}$, e.g. (10–40) °C, respectively. Heat and sink lines are separated by a minimum temperature difference $\Delta T_M = T_{M_{\text{heating}}} - T_{M_{\text{cooling}}} \geqslant$ (8–10) °C, which is required in order that cycle operation be possible. The higher this temperature difference, the better for cycle COP increase and complexity decrease. Unlike other known absorption cycles, most important feature of a truncated cycle is that in theory it is capable to process low temperature supplying sources forming heat/sink pairs of small temperature differences, e.g. $\Delta T_M =$ (10–50) °C, achieving cycle high temperature lift with very small power consumption ($COP_{\text{w}} = 50$ to 200), both in cooling and heating working mode. This is why, despite a higher complexity, which is conveniently chosen by the designer upon heat/sink sources availability, truncated cy-

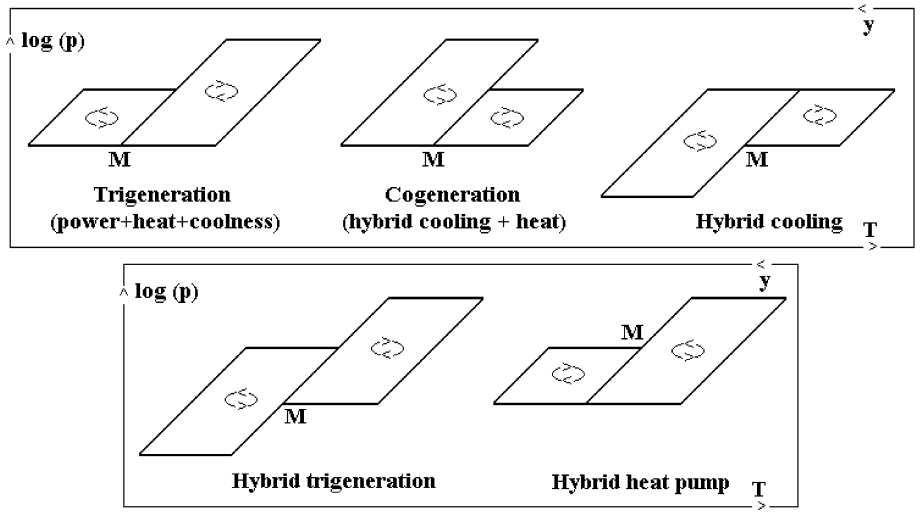

Fig. 7. Non-isobar nontruncated coabsorbent cycles.

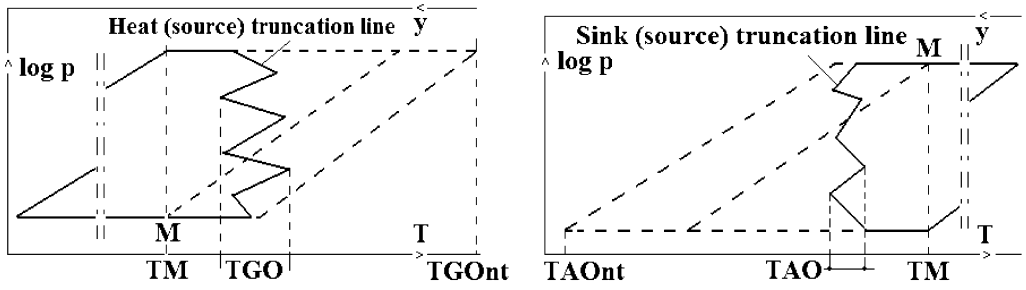

(a) (b)

Fig. 8. Truncation of the coabsorbent cycles: (a) cooling cycle; (b) heating cycle.

cles can have very important applications in clean heat pumping and power production. Nature and human industrial activity create such pairs of heat/sink sources, the problem is to identify and use them appropriately. One of the most attractive is that offered by a thermal power plant, where condenser cooling water and cooling tower cooled water could be truncated cycle heat/sink sources, respectively. Recent published works [5–15] emphasize these aspects describing for instance author proposal of using pure absorption and hybrid truncated cycles with ammonia/water in coupling with thermal power stations for most efficient district power, heat and cooling (trigeneration) in cities (power plant global efficiency higher than 0.9).

The truncation technique is described next [4,12,15]. A truncated cooling cycle is plotted by solid line in Fig. 9 in the $\log p - 1/T$ diagram (see also block flow chart). It comes of the nontruncated cooling cycle, represented by external contour with solid line in the left side and with dashed line in the right side. It includes a low pressure desorption process (1–2), p_l, e.g. (0.1–2) bar, where useful cooling effect occurs, e.g. $T_{DI} = (213.15–273.15)$ K and a truncation column having pressures between the low value and a high pressure p_n, e.g. (10–50) bar. Truncation column is made up by a low pressure absorption process (3–4) coupled on vapour side with the low pressure desorption process (1–2), a low pressure mixing process of absorbents coming of the low pressure absorption and desorption processes in order to generate the y_M one mean concentration and $T_M(p_l, y_M) \geqslant T_{M_{\text{cooling}}}$ temperature absorbent, point M, and a series of i stages, $i = 1, \ldots, n$, $n \in \mathbb{N}$, of isobar opposite intermediary generation $(5_i - 5_{GO,i})$ and resorption $(5_i - 5_{RO,i})$ processes, having increasing pressures, $p_n \geqslant p_{i+1} > p_i > p_l$ and temperatures between $T_{M_{\text{cooling}}}$ and $T_{M_{\text{heating}}}$ and being coupled on vapour side. Vapour have essentially increasing mean concentrations $Y_{G,m,i} \leqslant Y_{G,m,i+1} \leqslant Y_{G,m,n-1}$ and fulfil concentration threshold condition $y_{RO,i} \leqslant Y_{G,m,i}$, $i = 1, \ldots, n$. Stages are supplied in pre-established proportions by uniform absorbents coming, for the first stage of the mixture of the one mean concentration absorbent with that coming of the second generation stage, point 5_1, for each of the following next i stages of the mixture of the absorbent coming of the first inferior resorption stage $i - 1$ with that coming of the first superior generation stage $i + 1$, points 5_i, $i = 2, \ldots, n - 1$ (see arrows and detail A), and for the high pressure stage of the last but one resorption process $n - 1$, point 5_n. The truncation column has also processes between its successive stages, of the one mean concentration absorbent pressure increasing from p_l to p_1 and of the absorbent coming of resorption processes, p_{i-1} to p_i, $i = 2, \ldots, n$, of pressure reduction of absorbent coming of generation processes, from p_1 to p_l and from p_i to p_{i-1}, $i = 2, \ldots, n$, and of heat recovery between opposite processes of absorption–generation and of resorption–generation, of gax and of absorbent–absorbent type. Functionally, rich absorbent leaves truncation column last stage resorption process

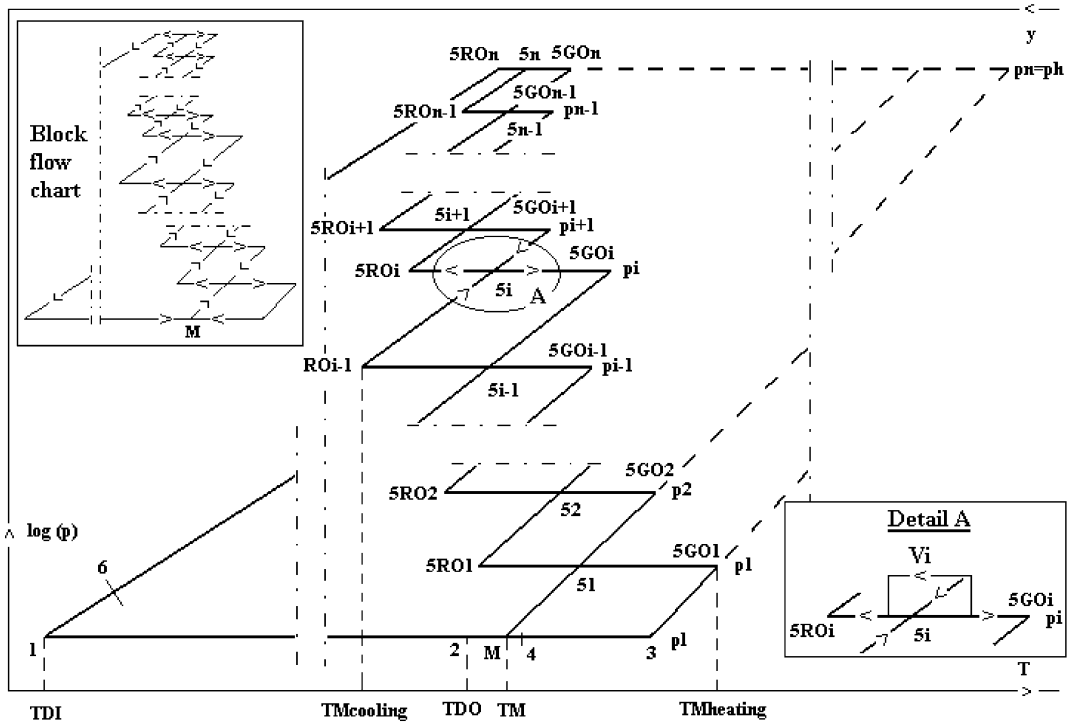

Fig. 9. The truncated cooling coabsorbent cycle.

$(5_n - 5_{RO,n})$ at p_n, is subcooled in a recovering way in the desorption process (1–2) at p_l from $T_{RO,n} \geqslant T_{M_{\text{cooling}}}$ till a temperature approaching T_{DI}, portion $(5_{RO,n} - 6)$, is expanded till p_l, it suffers the desorption process (1–2) where it extracts the heat from the medium which must be cooled and that of subcooling and reaches the state parameters $T_{DO} \leqslant T_M$ and $y_{DO} \geqslant y_M$, and the absorbent coming of the generation process $(5_1 - 5_{GO,1})$ of the first truncation column stage is subcooled in a recovering way, is expanded till the low pressure, it suffers the absorption process (3–4) of the desorbed refrigerent vapour, is mixed up at the low pressure with the absorbent coming of the desorption process and it generates the one mean concentration absorbent which is covering the truncation column in the way described above until the last stage at p_n, in order to close the cycle.

A truncated heating cycle is plotted by solid line in Fig. 10 (see also block flow chart). We shall not go into its details here, its description is given elsewhere [12,15].

We modelled both cooling and heating fractals having a same quadruple truncation column. Results are given in Fig. 11 [15], for cooling and heating (heat pump) power efficiency, COP_{w} (cooling or heating power/electrical power input), against desorber and resorber inlet temperatures, respectively, for same temperature gap $\Delta T_M = T_{M_{\text{heating}}} - T_{M_{\text{cooling}}} = 40\,^{\circ}\text{C}$ but differently placed in the low grade source region: A: $\Delta T = 50$–10; B: $\Delta T = 55$–15; C: $\Delta T = 60$–20; D: $\Delta T = 65$–25; E: $\Delta T = 70$–30; F: $\Delta T = 75$–35; G: $\Delta T = 80$–40; H: $\Delta T = 85$–45. For all A–H points cooling and heating, thermal efficiency (see Section 2.1) is $COP_{\text{c}} = 0.09951$–0.09684 and $COP_{\text{h}} = 0.2535$–0.2336, respectively, Fig. 11.

3.2. Truncation theory

A truncated coabsorbent cycle has particular topologic and flow properties, which determine its thermal behaviour. We shall emphasize these basic properties next, starting with the following:

Lemma 1. *Formally, graphically, representation of a* (*non*)*truncated heating* (*heat transformer*) *coabsorbent cycle in the* $\log p - 1/T$ *diagram can be obtained through an* $180°$ *plane rotation of the* (*non*)*truncated cooling coabsorbent cycle representation in same diagram.*

Proof. Indeed, rotating by $180°$ the graph of the (non)truncated cooling coabsorbent cycle shown in Fig. (1) 9, the representation of a (non)truncated heating coabsorbent cycle in same diagram is obtained, Fig. (4) 10. This is possible because all cycles loops (the "parallelograms" of the truncation column, made up by two adjacent isobars and isosteres) have same clockwise absorbent flow covering direction, which obviously is plane rotation free. □

This result will be used later. Another useful result is referring to a truncated cycle "anatomy" as follows:

Lemma 2. *A truncated cooling and heating* (*heat transformer*) *coabsorbent cycle can be obtained through the overlap of non-truncated coabsorbent cycles.*

Proof. Let us consider the truncated cooling coabsorbent cycle plotted in Fig. 12, a simpler version of Fig. 9, and isosteres passing through the points 9_i, $i = 2, \ldots, n-1$. With them, we

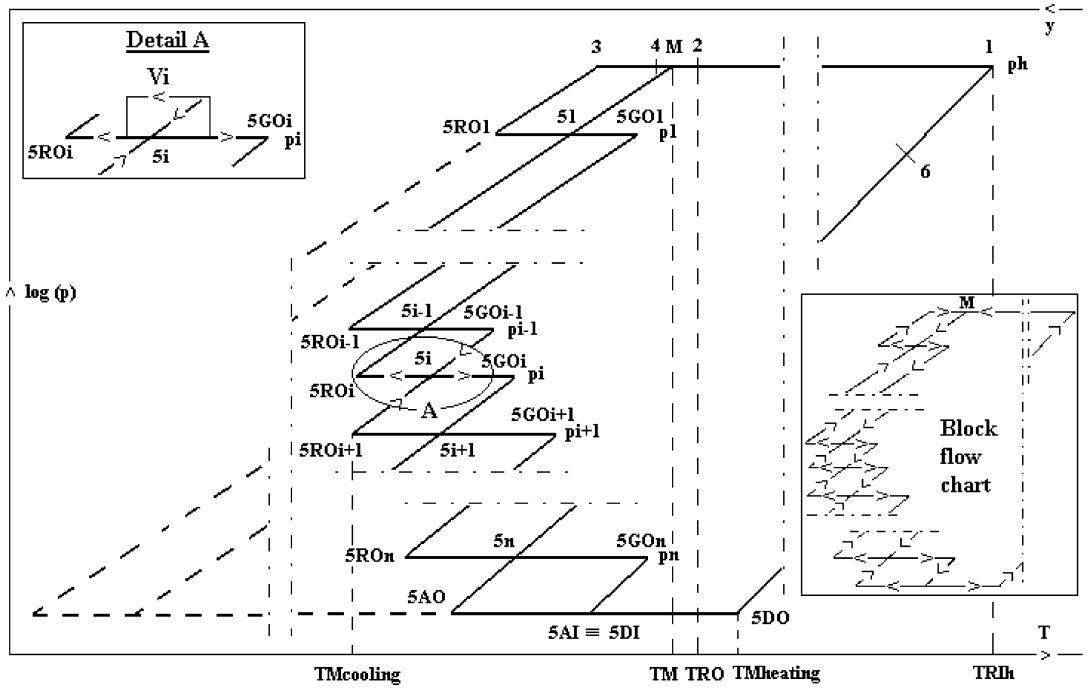

Fig. 10. The truncated heating (heat transformer) coabsorbent cycle.

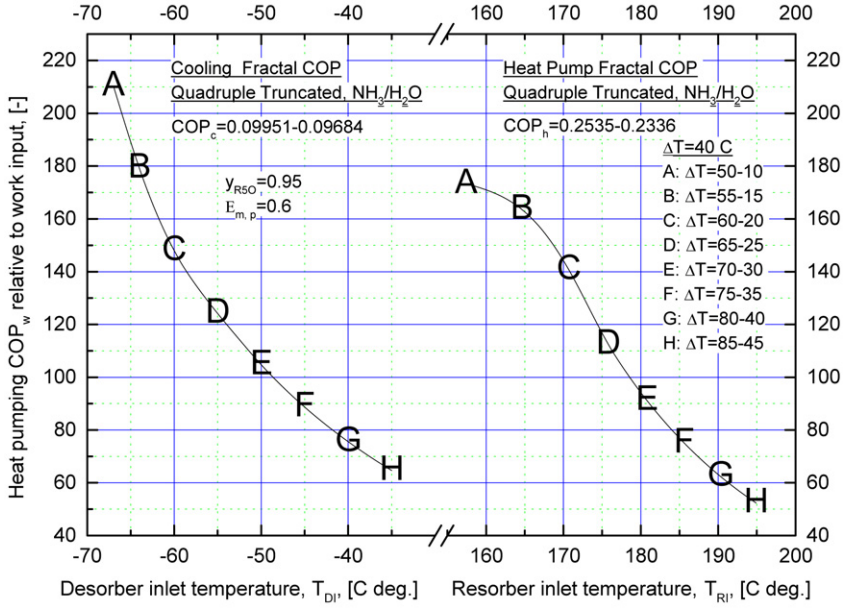

Fig. 11. Cooling and heating quadruple truncated fractal model results, giving cooling and heating (heat pump) COP_w, against desorber and resorber inlet temperatures, respectively, for same temperature gap of 40 °C but differently placed: A: $\Delta T = 50$–10; B: $\Delta T = 55$–15; C: $\Delta T = 60$–20; D : $\Delta T = 65$–25; E: $\Delta T = 70$–30; F: $\Delta T = 75$–35; G: $\Delta T = 80$–40; H: $\Delta T = 85$–45.

construct a sequence of three nontruncated cooling coabsorbent cycles noted as, Fig. 12: $(i+1)$: $M_{i+2}9_{i+1,r}9_{i+1}9_{i+1,g}M_i$; (i): $M_{i+1}9_{i,r}9_i9_{i,g}M_{i-1}$; $(i-1)$: $M_i9_{i-1,r}9_{i-1}9_{i-1,g}M_{i-2}$, and having as mixing points M_{i+1}, M_i and (i) cycle mixing isostere y_{M_i}. As a result, given the different pressure the three cycles are running on top with, p_{i-1}, p_i and p_{i+1}, with $p_{i-1} < p_i < p_{i+1}$, there will be three different portions of overlap on the y_{M_i} isostere, namely $M_i9_{i-1,r}$, with two overlaps, $9_{i-1,r}9_i$, with single overlap, and $9_i9_{i+1,g}$, with no overlap, respectively. We make now the remark that a mixing isostere is covered by a double absorbent flow, while the extreme isosteres of a nontruncated cycle are covered by a single absorbent flow, with an opposite direction as compared to that of the double absorbent flow. Bearing this and the above mentioned in mind, we can now infer that the two-overlap y_{M_i} isostere portion is vanishing, which reason for was represented by a dotted line in Fig. 12, and the single overlap portion becomes single flowed. This is why the single overlap and no overlap y_{M_i} isostere

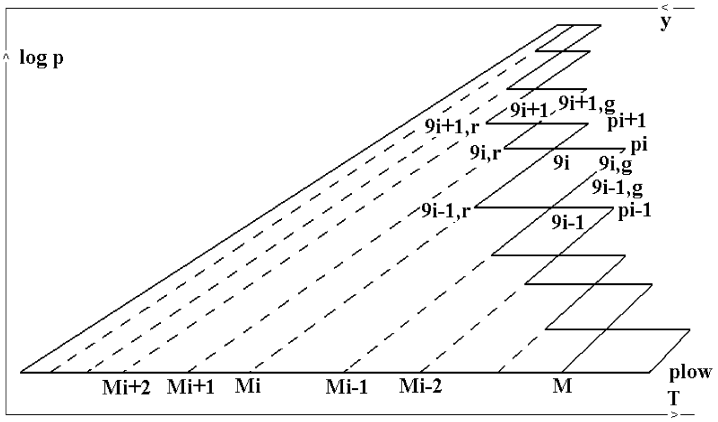

Fig. 12. A truncated cooling coabsorbent cycle build by nontruncated coabsorbent cycles overlap.

portions are operational and were consequently represented by solid lines. Extending our conclusion to the whole cycle, all two-overlap portions of the y_{M_i}, $i = 2, \ldots, n-1$, isosteres are vanishing, reason for which they were represented by dotted lines too. Concerning the y_{M_n} isostere, this is vanishing too, because here we do not have a two-overlap portion, and given the flow balance, it is covered by a single absorbent flow, which is counterbalanced by the $y_{n-1,r}$ counter-flow current. The y_M isostere is two-flow covered, as it results after a simple consideration, given the contribution of n-th desorber flow, which remains unbalanced because of the whole cycle p_{low} bottom vanishing, for the reasons outlined above. In this way, the whole cycle solid line has been proved, as resulting from nontruncated cycles overlap. □

Bearing in mind Lemma 1, we extend our conclusion to the truncated heating (heat transformer) coabsorbent cycles as well, and in this way the whole lemma has been proved. Not only a truncated coabsorbent cycle is topologic intrinsic related to a nontruncated cycle, as Lemma 2 showed, but these cycles have absorbent flow intrinsic similarities also, as it is stated by the following:

Lemma 3. *A truncated coabsorbent cycle, of cooling or heating (heat transformer) type, and its nontruncated coabsorbent cycle of origin, have same typical equation, which is independent of the truncation way.*

Proof. Let us first consider the truncated cooling coabsorbent cycle plotted in Fig. 9, which symbols of will be used hereinafter, together with those introduced for the nontruncated cycles in Section 2. We note outlet absorbent mass flow factors and each generation and resorption pressure stage vapour by:

$$g_{1,i} = \frac{Y_{G,i} - y_{GI,i}}{y_{GI,i} - y_{GO,i}}, \quad i = 1, \ldots, n \tag{41}$$

$$r_{1,i} = \frac{Y_{G,i} - y_{RI,i}}{y_{RO,i} - y_{RI,i}}, \quad i = 1, \ldots, n \tag{42}$$

and

$$V_i = \frac{V_{Gi}}{V_D}, \quad i = 1, \ldots, n \tag{43}$$

respectively. Mass balance on different parts of the cycle gives:

$$V_n r_{1,n} = d \tag{44}$$

$$V_1 g_{1,1} = a \tag{45}$$

$$(a_1 + d_1) + g_{1,2} V_2 = (r_{1,1} + g_{1,1}) V_1 \tag{46}$$

$$r_{1,i-1} V_{i-1} + g_{1,i+1} V_{i+1} = (r_{1,i} + g_{1,i}) V_i, \quad i = 2, \ldots, n-1 \tag{47}$$

$$r_{1,n-1} V_{n-1} = (r_{1,n} + g_{1,n}) V_n \tag{48}$$

Introducing Eqs. (44) and (45) in (46), using this result in first equation (47), and further on successively introducing the result of a precedent equation into the next one, it is obtained the recurrent equation

$$r_{1,i} V_i = g_{1,i+1} V_{i+1} + r_{1,n} V_n, \quad i = 1, \ldots, n-1 \tag{49}$$

With the help of recurrent equations (49), we eliminate step by step the $V_2, V_3, \ldots, V_{i-1}$ reduced vapour quantities of each cycle stage, and obtain

$$V_i \prod_{j=2}^{i} g_{1,j} = V_1 \prod_{j=1}^{i-1} r_{1,j} - r_{1,n} V_n \prod_{j=2}^{i-1} r_{1,j} \left(1 + \sum_{k=2}^{i-1} \prod_{j=2}^{k} s_j \right) \quad i = 2, \ldots, n-1 \tag{50}$$

where the s_j coabsorbent "j" stage symmetry factor is given by

$$s_j = \frac{g_{1,j}}{r_{1,j}} = \frac{y_{RO,j} - y_{M,j}}{y_{M,j} - y_{GO,j}}, \quad j = 1, \ldots, n \tag{51}$$

and $y_{M,j}$ is the coabsorbent "j" stage mixer concentration. In Eq. (50), we make $i = n$ in order to obtain

$$\frac{V_1}{V_n} = \frac{\prod_{j=2}^{n} r_{1,j}}{\prod_{j=1}^{n-1} r_{1,j}} \left(1 + \sum_{k=2}^{n} \prod_{j=2}^{k} s_j \right) \tag{52}$$

From Eqs. (44) and (45) we obtain

$$\frac{a}{d} = \left(\frac{V_1}{V_n} \right) \frac{g_{1,1}}{r_{1,n}} \tag{53}$$

and introducing Eq. (52) in Eq. (53) it results

$$\frac{a}{d} = \sum_{k=1}^{n} \prod_{j=1}^{k} s_j \tag{54}$$

In order to prove the first part of the lemma, we write Eq. (51) in the following form

$$s_j = \frac{\Delta y_{R,j}}{\Delta y_{G,j}}, \quad j = 1, \ldots, n \tag{55}$$

and remark that

$$\Delta y_{G,j} = \Delta y_{R,j-1}, \quad j = 2, \ldots, n \tag{56}$$

where from

$$\prod_{j=1}^{k} s_j = \frac{\Delta y_{R,k}}{\Delta y_{G,1}} \tag{57}$$

Using this result, Eq. (54) rewrites

$$\frac{a}{d} = \sum_{k=1}^{n} \prod_{j=1}^{k} s_j = \sum_{k=1}^{n} \frac{\Delta y_{R,k}}{\Delta y_{G,1}} = \frac{y_{RO} - y_M}{y_M - y_{GO}} = S \tag{58}$$

and the first part of the lemma has been proved. In order to prove its second part, we use Lemma 1. Indeed, rotating the truncated heat transformer coabsorbent cycle by 180 degrees, the obtained graph represent that of a truncated cooling coabsorbent cycle, for which the theorem was already proved, and in this way, taking into account that the truncation was chosen at random, the whole lemma is proved. The reduced vapour quantities of each cycle stage V_i, $i = 2, \ldots, n-1$, are obtained from Eq. (50), provided that that of the first stage, V_1, be chosen at convenience.

$$\begin{aligned} \frac{V_i}{V_1} &= \left(\frac{g_{1,1}}{g_{1,i}}\right) \frac{\sum_{k=i}^{n} \prod_{j=i}^{k} s_j}{\sum_{k=1}^{n} \prod_{j=1}^{k} s_j} = \left(\frac{g_{1,1}}{g_{1,i}}\right) \frac{1}{S} \sum_{k=i}^{n} \prod_{j=i}^{k} s_j \\ &= \frac{g_{1,1}}{g_{1,i}} \frac{(y_{RO} - y_{Mi})/(y_{Mi} - y_{GOi})}{(y_{RO} - y_M)/(y_M - y_{GO})} \\ i &= 1, \ldots, n \qquad \square \end{aligned} \tag{59}$$

The above results are conducting us to emphasize a more comprehensive nontruncated coabsorbent cycle property, expressed by the following:

Theorem. *The nontruncated cooling and heating (heat transformer) coabsorbent cycles are fractals from the topologic and absorbent flow point of view.*

Proof. According to Benoit Mandelbrot definition, every fragmented geometric shape, that is the truncated cycle, of a nontruncated cooling and heating (heat transformer) coabsorbent cycle, considered as a whole (origin), can be subdivided in parts, each of which, namely the nontruncated cycle, being a reduced size of the whole from the geometric point of view, according to Lemma 2, and behaves as a whole from the absorbent flow point of view, according to Lemma 3, and these statements proof the theorem. □

Theorem suggests the introduction of new shorted names for nontruncated cooling and heating coabsorbent cycles, such as *cooling and heating fractals*, respectively, used hereinafter.

3.3. Truncation columns, column cycles and comments

Finding truncation columns with minimum number of stages for a given task is a goal. Mixing points relative position determines such columns, plotted in Fig. 13(a), $\log p - 1/T$ diagram, for ammonia/water isobar stages and end generation and resorption temperatures equal to those of mixing points. Stages number increases with mixing points temperature difference decrease (from left to the right in figure). First left picture shows a nontruncated fractal, where temperature difference is high enough for cooling fractal mixing isostere be higher than that of the heating fractal. Decreasing temperature difference so that the two mixing isosteres overlap, as in second picture, the column results simple truncated. Further temperature difference decrease makes heating fractal mixing isostere have increasingly higher values as that of the cooling fractal one, and truncated columns increase complexity to double, triple, quadruple-truncated, etc. When stages processes are non-isobar (see plate heat exchangers use as mass and heat exchangers), the column becomes non-isobar, Fig. 13(b).

The "height" of a truncation column is expressed by:

$$h_t = \frac{y_{RO,n} - y_{GO,1}}{T_{RO,n} - T_{GO,1}} \tag{60}$$

Low generation temperatures with high sink temperatures in the cooling operation and high resorption temperatures with low heat temperatures in the heating operation lead to high columns use, which require an increased number of loops, typically three to five for ammonia/water, and have column index values in the range of $h_t = 0.02$–$0.03\ \mathrm{K}^{-1}$.

Integrating a truncation column in a closed circuit may result in a *power column cycle*, Fig. 14(a), with clockwise covered loops and a turbo-generator connected between column top and bottom, or in a *heat pump column cycle*, Fig. 14(b), with loops covered counter-clockwise and a compressor connected between column top and bottom. These cycles are analyzed elsewhere [9,14].

A comment on truncated cycle introduction follows, based on cooling working mode with ammonia/water. Single-stage condensation cycle works with pure absorption and has 4 devices, a pump, two heat exchangers and a rectification device. For high temperature lifts and low heat source temperature supply, $T_{GO} > 80\,^{\circ}\mathrm{C}$, two stage cycle is used [17], which adds 2 more devices, a pump and a heat exchanger. Two stage cycle has absorbent inventory problems, working for this reason discontinuously, and a low COP, e.g. 0.2–0.3, equal to useful effect energy output divided by the input of quality energy ((generation + rectification) heats + pumping work). A full truncated cycle works with pure absorption as well, but continuously, as a first great practical advantage because it has not absorbent inventory problem, and lacks vapour rectification, as a second advantage. It has 2 devices and a heat exchanger, and depending on the desired useful cooling effect temperature, it needs 3 to 5 isobar stages with a total of 6 to 10 resorption and generation, for heat/sink pair temperature differences of $\Delta T_M = \max 40\,^{\circ}\mathrm{C}$. One pump and one heat exchanger is added also for each isobar stage. It has as energy input (see Fig. 11), heat of a low temperature potential, usually free, COP_{c} and COP_{h} are less unity

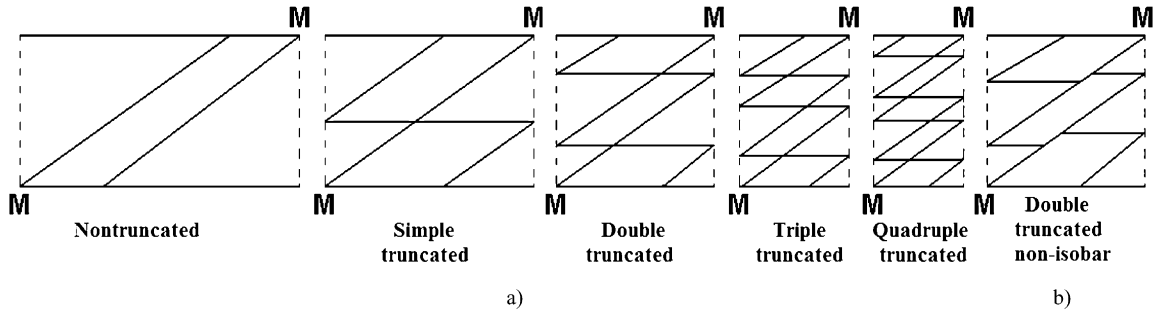

Fig. 13. (a) The dependence of the minimum stages number of an isobar truncation column (a) on the cooling and heating fractals mixing points relative position; (b) Non-isobar truncation column.

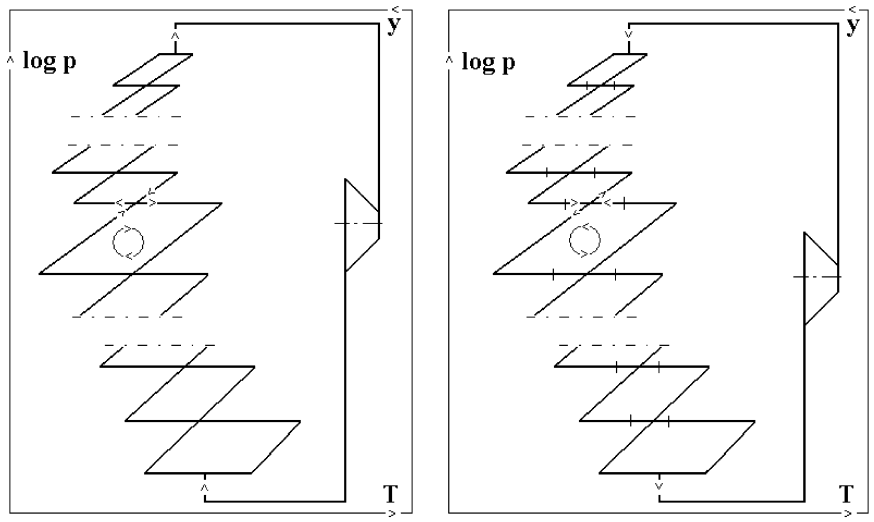

Fig. 14. Column cycles: (a) power cycle and (b) hybrid heat pump cycle.

and COP_w is very high ($COP_w = 50$ to 200). From the above, on one side, full truncated cycle has maximum complexity and COP_w value. On the other side, Osenbrück cycle, with hybrid operation, is the simplest one, with only two devices, a pump, a compressor, a heat exchanger, has minimum COP_w value, because of highest compression ratio and uses same heat sources, but at higher COP_c and COP_h. Non-isobar coabsorbent cycles, can be truncated as well (see Fig. 7, Table 4 and [12]), obtaining the hybrid operation truncated cycles, potentially very useful in practice. They fill the gap between cycles mentioned above with extreme complexity and COP_w values. Hybrid truncation use is indicated when sources availability is limited, or when cycle complexity must be decreased. The degree of truncation can be chosen at convenience, in order to reach better feasibility over other systems. Hybrid nontruncated and simple truncation seems to offer satisfactory low complexity and still high COP_w, because truncated column introduction considerably diminish compression ratios. Results of hybrid operation are given for truncated cycles in, e.g. [7,9,12–15]. Just to show the high potential of these cycles we give in Table 4 some comparative COP_w values of mechanical vapour compression versus non-isobar hybrid truncated cycles in cooling working mode. Input data in Table 4 are: sink at 30 °C, heat at 70 °C ($\Delta T_M = 70–30 = 40$ °C), hybrid nontruncated and simple truncation.

3.4. Fractals COP

This paragraph deals with the first and second law COP assessment of the coabsorbent cycles presented so far. They are given in Table 5. Details concerning calculation are given in Appendix A.

3.5. External coabsorbent cycle composition

One of most interesting application here is to transpose advanced (multi-effect) cycles in coabsorbent technology, made according to the: *Rule of transposition in coabsorbent cycles* [1]: *A separate absorbent condensing cycle of origin can be transposed in a coabsorbent cycle, if condensing cycle subcycles of cascade were replaced each by a nontruncated coabsorbent cycle* (*fractal*)*, and then interconnected, more often than not through their superposition, provided that at least a mixing point exists.* New, simplest, application interesting cycles, obtained through external nontruncated cycle composition, are derived by adding a convenient number of pressure (Fig. 15(A)–(C)) or concentration (Fig. 15(D)–(F)) stages to a

Table 4
Comparative cooling COP_w values of ammonia mechanical vapour compression versus hybrid truncated cycles with ammonia/water working combination

Cooling type	Industrial cooling, −45 °C	Medium cooling, −22.5 °C	Air conditioning, 0 °C
Classic mechanical vapour compression cooling (practice)	1.26 (CO_2/ammonia cascade)	1.96	3.63
Hybrid truncated cooling cycles* (calculated)	3.69 (5.17)** Hybrid simple truncated	11.56 Hybrid simple truncated	33.2 Hybrid nontruncated

* Cycles produce simultaneously heat as well, at 50 to 140 °C;
** $\Delta T_M = 85–32 = 53$ °C.

Table 5
Cooling and heating first and second law COP of fractals truncated fractals, hybrid fractals and hybrid fractals cascades

Cycle	First law	Second law
Cooling fractal	$COP_{\mathrm{cf}} = \dfrac{q_D}{q_G}$	$COP_{C,\mathrm{cf}} = \eta_w COP_q = \dfrac{q_D}{q_G} = \left(1 - \dfrac{T_{RO}}{T_{GO}}\right)\left(\dfrac{T_{AI}}{T_{DI}} - 1\right)^{-1}$
Heating fractal	$COP_{\mathrm{hf}} = \dfrac{q_R}{q_G + q_D}$	$COP_{C,\mathrm{hf}} = \left(\left(1 - \dfrac{T_{AO}}{T_{DO}}\right)^{-1}\left(1 - \dfrac{T_{GI}}{T_{RI}}\right) + \dfrac{T_{GI}}{T_{RI}}\right)^{-1}$
Truncated cooling fractal	$COP_{\mathrm{tcf}} = q_D\left[\sum_{i=1}^{n} q_{G,i}\dfrac{1-(T_{R,i}/T_{G,i})}{(1-T_R/T_G)_{\max}} + w_{\mathrm{pump}}\right]^{-1}$	$COP_{C,\mathrm{tcf}} = \dfrac{q_D}{q_G} = \dfrac{\sum_{i=1}^{n} q_{D,i}}{\sum_{i=1}^{n} q_{G,i}} = \dfrac{\sum_{i=1}^{n} q_{G,i}(1-T_{RO,i}/T_{GO,i})(T_{AI,i}/T_{DI,i}-1)^{-1}}{\sum_{i=1}^{n} q_{G,i}}$
Truncated heating fractal	$COP_{\mathrm{thf}} = q_{R,1\text{–}2}\left(1-\dfrac{T_R}{T_G}\right)_{\max} \times\left[\left(\sum_{i=1}^{n} q_{G,i}\left(1-\dfrac{T_{R,i}}{T_{G,i}}\right) + q_D\left(1-\dfrac{T_{AO}}{T_{DO}}\right)\right) + w_{\mathrm{pump}}\left(1-\dfrac{T_R}{T_G}\right)_{\max}\right]^{-1}$	$COP_{C,\mathrm{thf}} = \dfrac{q_{R,1\text{–}2}}{\sum_{i=1}^{n} q_{G,i} + q_D} = \left[\dfrac{T_{RI,1\text{–}2}}{(T_{RI,1\text{–}2} - T_{GI,3\text{–}4})}\sum_{i=1}^{n} q_{G,i}\left(1-\dfrac{T_{RO,i}}{T_{GO,i}}\right) + q_D\left(1-\dfrac{T_{AO}}{T_{DO}}\right)\right]\left[\sum_{i=1}^{n} q_{G,i} + q_D\right]^{-1}$
Hybrid cooling fractal	$COP_{\mathrm{hcf}} = \dfrac{q_D}{w_c + w_{\mathrm{pump}}}$	$COP_{C,\mathrm{hcf}} = \dfrac{q_D}{\lvert w_c\rvert} = \left\lvert\left(\dfrac{T_{AI}}{T_{DI}} - 1\right) - \dfrac{1}{q_D}\sum_{i=1}^{m} q_{G,i}\left(1-\dfrac{T_{RO,i}}{T_{GO,i}}\right)\right\rvert^{-1}$
Hybrid heating fractal	$COP_{\mathrm{hhf}} = \dfrac{q_R}{w_c + w_{\mathrm{pump}}}$	$COP_{C,\mathrm{hhf}} = \dfrac{q_R}{\lvert w_c\rvert} = \left\lvert\left(1-\dfrac{T_{GI,3\text{–}4}}{T_{RI,1\text{–}2}}\right) - \dfrac{1}{q_R}\left(\sum_{i=1}^{m} q_{G,i}\left(1-\dfrac{T_{RO,i}}{T_{GO,i}}\right) + q_D\left(1-\dfrac{T_{AO}}{T_{DO}}\right)\right)\right\rvert^{-1}$
Hybrid cooling and heating fractal cascade	$COP_{\mathrm{c},IJ} = \dfrac{IJ}{I+J+1}$; $COP_{\mathrm{h},IJ} = \dfrac{IJ}{I+J-1}$; $COP_{\mathrm{c},IKL} = \dfrac{IKL}{I+K+L+IK+IL+KL+1}$; $COP_{\mathrm{h},IKL} = \dfrac{IKL}{IK+IL+KL-I-K-L+1}$	

basic fractal. Mixing points are noted by M and upset M for cooling and heating fractals, respectively. Out of these, cooling cycle with pressure stages will be analyzed here, as it can operate with both broad and narrow solubility field working combinations, has simpler flow (require one mixing point only), is less complex and is efficient. The two last aspects will be emphasized next.

Transposition has practical importance: (I) Punctual condensing is replaced by resorption working on a larger temperature range. This diminishes heat exchange exergy loss and has impact on cycle COP. We consider here just the n pressure stages cooling cycle, origin versus transposed, but conclusion covers heating cycle as well. COP of origin advanced cycle has expression

$$COP_{\mathrm{acc,cond}} = \sum_{i=k}^{n}\prod_{j=1}^{k}\eta_j \tag{107}$$

In Eq. (107), obtained first by [21] for up to triple-effect and extended later for higher-order effects by [22], η_j are cooling COP's of cascade subcycles, which normally have different values, as work with different parameters. Eq. (107) shows that an investment for COP increase, through adding new effects to cas-

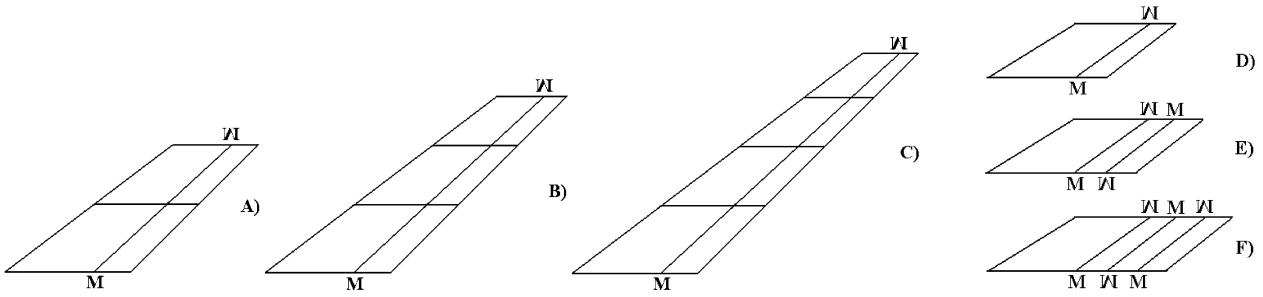

Fig. 15. New coabsorbent cycles with double (A), triple (C) and quadruple (C) pressure stages and with simple (E) and double (F) concentration stages, $\log p - 1/T$ diagram.

cade, therefore increasing complexity, has diminished returns. On contrary, transposed advanced cycle shows investment for COP increase will have proportional expected returns, because replacing condensing by resorption, rejected available heat is usually higher than condensing heat, comparable to that of its vapour coupled generation for symmetry factors sensibly equal to unity, that is we shall have rather a linear expression

$$COP_{\text{acc,coabs}} = \sum_{i=1}^{n} \eta_i \tag{108}$$

as cycle COP than that given by Eq. (107), where η_i, $i = 1, \ldots, n$, are basically the COP's of each cooling fractal of the cascade. (II) Large overlapping temperature met in resorption/generation gax recovery use, enables comparative heat source temperature decrease and cycle exergy COP increase. This is why, a transposed cycle can usually have one more added effect, as compared to its origin cycle, for same maximum operating temperature [10,14]. (III) Complete elimination of vapour rectification in the volatile absorbent working combinations operation favours again cycle COP. (IV) Transposed cycle has less main component devices as its origin. Indeed, this time same role and same working parameters devices of different subcycles can be replaced by a single one of equivalent capacity, without any absorbent inventory problem risk. For a n_{effect} cycle, out of the total of $4n_{\text{effect}}$ main devices, $2(n_{\text{effect}} - 1)$ have same function (absorbers and desorbers) and working parameters and can be replaced by those belonging to the basic fractal with corresponding capacity, so only $2(n_{\text{effect}} + 1)$ main devices remain for achievement. Next we shall go deeper into this cycle through the following:

Lemma 4. *Pressure stages coabsorbent cycle resulted from transposition of a n-effect advanced absorption cycle recovering condensing heat, has absorption and desorption absorbent flow factors as*

$$a = V_1 \sum_{i=1}^{n} g_{1,i} \prod_{j=1}^{i-1} r_{\text{gax},j} \tag{109}$$

and

$$d = V_1 \sum_{i=1}^{n} r_{1,i} \prod_{j=1}^{i-1} r_{\text{gax},j} \tag{110}$$

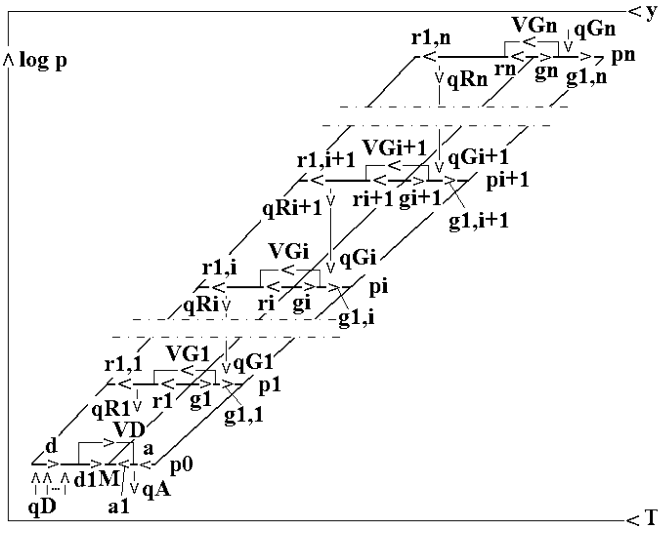

Fig. 16. A n-effect cooling cycle with condenser heat recovery, transposed into a (coabsorbent) pressure stages cooling fractal.

respectively, and same characteristic equation as that of basic cooling fractal, where $r_{\text{gax},i}$, $i = 1, \ldots, n-1$, *are* gax *factor of* $(i+1)$*-th resorption process yielding heat to the* i*-th generation internal heat recovering process.*

Proof. Let us consider the coabsorbent cycle, plotted in the $\log p - 1/T$ diagram in Fig. 16, resulting from adding p_i, $i = 1, \ldots, n$, pressure stages to the basic bottom cooling fractal, working between p_0 and p_1 pressures and $y_{RO,1}$ and $y_{GO,1}$ extreme concentrations, with y_M mixing concentration. Mass balances on absorption and desorption processes, as well as a heat balance on the $(i+1)$-th and i-th pressure stage gax heat exchange, $i = 1, \ldots, n-1$, results in

$$a = \sum_{i=1}^{n} V_i g_{1,i} \tag{111}$$

and

$$d = \sum_{i=1}^{n} V_i r_{1,i} \tag{112}$$

and

$$q_{R,i+1} = q_{G,i} \tag{113}$$

respectively, where $V_i, i = 1, \ldots, n-1$, is given by Eq. (43), and

$$q_{R,i} = V_{G,i} q_{R,u,i} \tag{114}$$

with

$$q_{R,u,i} = (I_{G,i} - i_{RI,i}) + r_{1,i}(i_{RI,i} - i_{RO,i}) \tag{115}$$

and

$$q_{G,i} = V_{G,i} q_{G,u,i} \tag{116}$$

with

$$q_{G,u,i} = (I_{G,i} - i_{GI,i}) + g_{1,i}(i_{GO,i} - i_{GI,i}) \tag{117}$$

From Eqs. (113)–(117), we obtain

$$V_{i+1} = V_i r_{\text{gax},i} \tag{118}$$

where

$$r_{\text{gax},i} = \frac{q_{G,u,i}}{q_{R,u,i+1}} \tag{119}$$

is gax factor of $(i+1)$-th resorption process yielding heat to the i-th generation internal heat recovering process, $i = 1, \ldots, n-1$. In recurrent equation (118) we make successively $i = 1, 2, \ldots, i-1$, in order to find

$$V_i = V_1 \prod_{j=1}^{i-1} r_{\text{gax},j}, \quad i = 1, \ldots, n-1 \tag{120}$$

Similarly to Lemma 3, we choose V_1 and remark that $V_i > V_{i+1}, i = 1, \ldots, n-1$, because $r_{\text{gax},j} < 1$, for all j, where from it results that V_1 has highest value amongst all other stages reduced vapour. With Eq. (120), Eqs. (111) and (112) become Eqs. (109) and (110), and first part of lemma has been proved. In order to prove its second part, it suffices to multiply and divide $g_{1,i}$ in Eq. (109) by $r_{1,i}$, and remark that

$$\frac{g_{1,i}}{r_{1,i}} r_{1,i} = \frac{g_{1,1}}{r_{1,1}} r_{1,i} = S r_{1,i}, \quad i = 1, \ldots, n \tag{121}$$

wherefrom, introducing this result in Eq. (109), we obtain

$$a = S V_1 \sum_{i=1}^{n} r_{1,i} \prod_{j=1}^{i-1} r_{\text{gax},j} = Sd \tag{122}$$

or

$$\frac{a}{d} = S \tag{123}$$

which proofs the whole lemma. The cycle first law cooling COP is given by

$$COP_{\text{psccac}} = \frac{q_D}{q_{G,n}} = \frac{q_{D,u}}{V_n q_{G,u,n}} = q_{D,u} \left(V_1 q_{G,u,n} \prod_{j=1}^{n-1} r_{\text{gax},j} \right)^{-1} \tag{124}$$

where

$$q_D = V_D q_{D,u} \tag{125}$$

and

$$q_{D,u} = (I_D - i_{DO}) + d(i_{DO} - i_{DI}) \tag{126}$$

Lemma 4 was applied to model transposed double-effect and quadruple-effect cooling coabsorbent cycles for NH_3/H_2O and H_2O/LiBr, which results of are given in Fig. 17 (a) and (b), respectively. Results confirm points (I)–(VI). In case of NH_3/H_2O, comparatively, double-effect is possible within condensing absorption at 2–3 times higher working pressures in the high temperature generator and with much lower COP because especially of rectification need. Here, COP_c is completely verified by Eq. (108), for $\eta_i = 0.35$–0.50, Fig. 17(a). Same Fig. 17(a) shows also co-generated heating effect COP_h, not present in condensing absorption. In case of H_2O/LiBr, Fig. 17(b), COP_c is placed between values given by Eqs. (107) and (108), if most probable $\eta_i = 0.72$ value were considered for this combination. Same additional heating effect is quantified in this case as well. Internal heat exchange used for model these cycles is given elsewhere [14]. Number of main devices to be manufactured is 6 instead of 8 for double-effect NH_3/H_2O and 10 instead of 16 for quadruple-effect H_2O/LiBr. Comparative heat source temperature decrease results as well from T_{G2O} and T_{G4O} plots. □

4. Conclusions

The paper presents further research results in coabsorbent cycles. After introduction, isobar and non-isobar nontruncated cooling and heating coabsorbent cycles are analyzed, emphasizing advantages they could bring in absorption technology: a) elimination of vapour rectification need; b) elimination of absorbent inventory problem; c) increase of cycle match with gliding sources; d) non-condensable refrigerant operation capacity; e) favouring behaviour for control and optimization; f) gax effect use and cycle exergy efficiency increase favouring; g) cycle complexity decrease; h) capacity to transpose known condensation absorption cycles, and create new ones. Further, new simplest coabsorbent cycles with potential applications are proposed, derived through nontruncated internal and external cycles composition. Truncation method, theory and columns are described within internal composition, stressing truncated cycles capacity to match better sources with tasks in applications. First and second law COP's are also given for presented cycles. New cycles with pressure and concentration stages resulting from external composition are introduced. Transposition of condensation n-effect cooling cycle with condenser heat recovery, by pressure stages coabsorbent cycles, is analyzed. Each new cycle introduced is modelled and results thereof are shortly presented by plots and comments.

Appendix A

Cooling Fractal COP: The COP estimate will be done in relation with Fig. 1. For the Carnot COP it is considered that isobar generation–resorption process produces the w ideal maximum mechanical work, according to

$$\eta_w = \frac{w}{q_G} = \frac{q_G - q_R}{q_G} = 1 - \frac{T_{RO}}{T_{GO}} \tag{A.1}$$

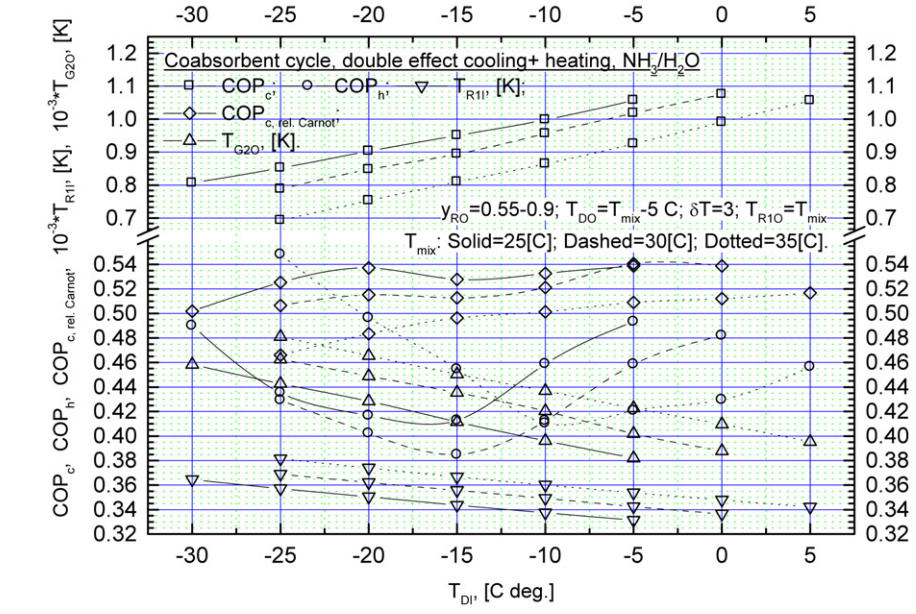

(a)

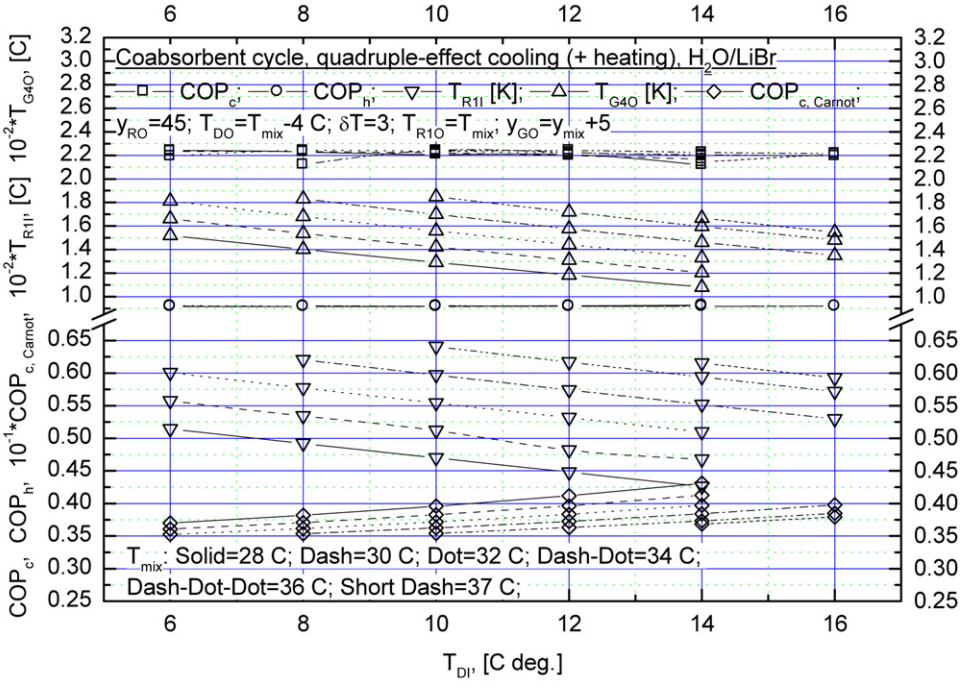

(b)

Fig. 17. Coabsorbent transposed model results of advanced cycle shown in Fig. 16: (a) NH_3/H_2O double-effect cooling and quadruple-effect H_2O/LiBr air conditioning, against desorber inlet temperature.

which is used to power the ideal isobar desorption–absorption cooling process for a maximum efficiency useful effect q_D, as

$$COP_q = \frac{q_D}{w} = \frac{q_D}{q_A - q_D} = \left(\frac{T_{AI}}{T_{DI}} - 1\right)^{-1} \tag{A.2}$$

wherefrom, equation in Table 5 results.

Heating fractal COP: The COP estimate will be done in relation with Fig. 4. For Carnot COP, it will be considered that isobar desorption–absorption process produces the w ideal maximum mechanical work, according to

$$\eta_w = \frac{w}{q_D} = \frac{q_D - q_A}{q_D} = 1 - \frac{T_{AO}}{T_{DO}} \tag{A.3}$$

which is used to power the ideal isobar generation–resorption heating process for a maximum efficiency useful effect q_R, upgrading the q_G heat extracted in the generation process

$$COP_q = \frac{q_R}{w} = \frac{q_R}{q_R - q_G} = \frac{T_{RI}}{T_{RI} - T_{GI}} \tag{A.4}$$

The Carnot COP is calculated like to the heat transformer, by

$$COP_{C,\mathrm{hf}} = \frac{q_R}{q_G + q_D} = \left(\frac{q_G}{q_R} + \frac{q_D}{q_R}\right)^{-1} \tag{A.5}$$

where the first and second ratio in Eq. (A.5) result from Eqs. (A.4) and (A.3) and (A.4) as

$$\frac{q_G}{q_R} = \frac{T_{GI}}{T_{RI}} \tag{A.6}$$

and

$$\frac{q_D}{q_R} = (\eta_w COP_q)^{-1} = \left(1 - \frac{T_{AO}}{T_{DO}}\right)^{-1}\left(1 - \frac{T_{GI}}{T_{RI}}\right) \tag{A.7}$$

respectively. Introducing Eqs. (A.6) and (A.7) in (A.5), equation in Table 5 results.

Truncated cooling fractal COP: The COP estimate will be done in relation with Fig. 9. For Carnot COP it is considered that i-th isobar generation–resorption process produces the $w_i, i = 1, 2, \ldots, n$, ideal maximum mechanical work, according to

$$\eta_{w,i} = \frac{w_i}{q_{G,i}} = \frac{q_{G,i} - q_{R,i}}{q_{G,i}} = 1 - \frac{T_{RO,i}}{T_{GO,i}} \tag{A.8}$$

which is used to power its shear of the ideal isobar desorption–absorption cooling process for a maximum efficiency useful effect $q_{D,i}$, as

$$COP_{q,i} = \frac{q_{D,i}}{w_i} = \frac{q_{D,i}}{q_{A,i} - q_{D,i}} = \left(\frac{T_{AI,i}}{T_{DI,i}} - 1\right)^{-1} \tag{A.9}$$

wherefrom it results that thermal Carnot efficiency for this shear would be

$$\begin{aligned} COP_{C,i} &= \frac{q_{D,i}}{q_{G,i}} = \eta_{w,i} COP_{q,i} \\ &= \left(1 - \frac{T_{RO,i}}{T_{GO,i}}\right)\left(\frac{T_{AI,i}}{T_{DI,i}} - 1\right)^{-1} \end{aligned} \tag{A.10}$$

Equation in Table 5 results now using Eq. (A.10). For multi-temperature source generation supply, first law COP takes into account not only quantity, but quality of cycle each individual generation heat input $q_{G,i}, i = 1, 2, \ldots, n$, as well, wherefrom equation in Table 5 results.

Truncated heating fractal COP: The COP estimate will be done in relation with Fig. 10. For Carnot COP, it will be considered that isobar desorption–absorption process produces the w_{AD} ideal maximum mechanical work, according to

$$\eta_{w_{AD}} = \frac{w_{AD}}{q_D} = \frac{q_D - q_A}{q_D} = 1 - \frac{T_{AO}}{T_{DO}} \tag{A.11}$$

and i-th isobar generation–resorption process produces the $w_i, i = 1, 2, \ldots, n$, ideal maximum mechanical work, according to

$$\eta_{w,i} = \frac{w_i}{q_{G,i}} = \frac{q_{G,i} - q_{R,i}}{q_{G,i}} = 1 - \frac{T_{RO,i}}{T_{GO,i}} \tag{A.12}$$

Ideal mechanical works $w_i, i = 1, 2, \ldots, n$, and w_{AD} are used to power ideal isobar resorption–generation heating process (states 1–2 and 3–4, respectively) for a maximum efficiency useful effect $q_{R,1\text{–}2}$, upgrading $q_{G,3\text{–}4}$ heat extracted in the generation process (states 1–2)

$$\begin{aligned} COP_q &= \frac{q_{R,1\text{–}2}}{\sum_{i=1}^{n} w_i + w_{AD}} = \frac{q_{R,1\text{–}2}}{q_{R,1\text{–}2} - q_{G,3\text{–}4}} \\ &= \frac{T_{RI,1\text{–}2}}{T_{RI,1\text{–}2} - T_{GI,3\text{–}4}} \end{aligned} \tag{A.13}$$

Equation in Table 5 results with the help of Eqs. (A.11)–(A.12). First law COP estimate of truncated heating fractal is confronted with cycle multi-temperature source generation supply, similarly to the truncated cooling fractal, so we will proceed in the same way and equation in Table 5 results.

Hybrid cooling and heating fractals COP: First we shall calculate the Carnot COP of a hybrid cooling fractal. The COP will be assessed for the practical case, when heat input can be neglected, but not the mechanical work input. A whole truncated column would have produced in its i-th isobar generation–resorption process the $w_i, i = 1, 2, \ldots, n$, ideal maximum mechanical work, according to

$$\eta_{w,i} = \frac{w_i}{q_{G,i}} = \frac{q_{G,i} - q_{R,i}}{q_{G,i}} = 1 - \frac{T_{RO,i}}{T_{GO,i}} \tag{A.14}$$

with a total mechanical work produced, resulting from Eq. (A.14), of

$$\sum_{i=1}^{n} w_i = \sum_{i=1}^{n} q_{G,i}\left(1 - \frac{T_{RO,i}}{T_{GO,i}}\right) \tag{A.15}$$

This work powers the ideal isobar desorption-absorption cooling process for a maximum efficiency useful effect q_D, as

$$COP_q = \frac{q_D}{\sum_{i=1}^{n} w_i} = \frac{q_D}{q_A - q_D} = \left(\frac{T_{AI}}{T_{DI}} - 1\right)^{-1} \tag{A.16}$$

If now the ideal maximum mechanical work were produced by a m stage column, with $m < n$, the rest of the mechanical work must be supplied by the ideal compressor, that is

$$w_c = \sum_{i=1}^{n} w_i - \sum_{i=1}^{m} w_i \tag{A.17}$$

or, otherwise expressed with Eqs. (A.15) and (A.16),

$$|w_c| = \left| q_D\left(\frac{T_{AI}}{T_{DI}} - 1\right) - \sum_{i=1}^{m} q_{G,i}\left(1 - \frac{T_{RO,i}}{T_{GO,i}}\right)\right| \tag{A.18}$$

The Carnot COP of a hybrid cooling fractal can be assessed now, bearing in mind the remark we made in the beginning of this paragraph, and equation in Table 5 results. Carnot COP of a hybrid heating fractal can be assessed similarly, and equation in Table 5 results.

COP of hybrid cooling and heating fractals cascades: When a cycle cooling/heating source temperature is two high/low for a given application, two same type cycles can be coupled in a cascade, in order to accomplish the cooling/heating task. The prize paid for this known technical solution is an always lower COP of the compound as compared to the components COP's, because the first cycle useful effect is no more in fact the desired final effect, but becomes cooling or heating source for the

second cycle in case of the cooling and heating cascades, respectively, and last but not the least, the compound complexity increases. Supposing we have two hybrid cooling fractals with COP's equal to "I" and "J", respectively, and same holds true for two hybrid heating fractals, the cooling and heating cascades have the compound COP's given by first two equations in Table 5, respectively, which can be easily proved, starting from equations of first law hybrid cooling and heating fractals in Table 5 and taking into account the cascade condition. Also, these equations can be used step by step in order to further calculate multi-component cascades COP's. Indeed, if for instance "J" resulted from a cascade of "K" and "L" COP's, then the two last equations in Table 5 result for three-component cascades.

References

[1] M.D. Staicovici, Coabsorbent cycles, in: Proceedings of the Gustav Lorentzen Natural Working Fluids Conference, Trondheim, Norway, 2006 May 28–31, pp. 219–222.
[2] M.D. Staicovici, Heat pump, Romanian patent file deposition No. A/00135/02.03.2006, 2006 (in Romanian).
[3] M.D. Staicovici, Coabsorbent hybrid cooling plant, Romanian patent file deposition No. A/00588/24.07.2006, 2006 (in Romanian).
[4] M.D. Staicovici, Truncated coabsorbent cycle cooling method and application plant, Romanian patent file deposition No. A/00748/26. 09.2006, 2006 (in Romanian).
[5] M.D. Staicovici, The coabsorbent cycle technology for heat pumping applications, Presented to the "Confort, efficiency, energy conservation and environment protection", UTCB Conference, 29–30 Nov., 2006, Bucharest, Romania.
[6] M.D. Staicovici, Coabsorbent heat pumping method by coupling with a thermal power station and application plant, Romanian patent file deposition No. A/00134/22.02.2007, 2007 (in Romanian).
[7] M.D. Staicovici, Coabsorbent cycle technology for ammonia/water heat pumping applications, in: Proceedings of the "Ammonia Refrigeration Technology for Today and Tomorrow" IIR Conference, April 19–21, 2007, Ohrid, Macedonia.
[8] M.D. Staicovici, Coabsorbent heat pumps for the future, IEA-Heat Pumps Newsletter 25 (1) (2007) 29–32.
[9] M.D. Staicovici, Coabsorbent cycle technology for low grade sources thermal recovery, in: Proceedings of the "Technological Innovations in Air Conditioning and Refrigeration Industry" XII European Conference, vol. I–II, Milan, June 2007.
[10] M.D. Staicovici, Coabsorbent technology for heat pumping applications, in: Proceedings of the IIRIIF 22 International Congress of Refrigeration, E1-2-1039, Beijing, 2007.
[11] M.D. Staicovici, Coabsorbent technology for future cooling applications, Sent to Rajendra Shende, Director of the United Nations Environment Programme (UNEP), July 2007, and Didier Coulomb, Director of the International Institute of Refrigeration, November 2007, 2007.
[12] M.D. Staicovici, Coabsorbent cycles heat pumping and mechanical work producing procedure and applying installation, International patent file deposition No. PCT/RO 2007/000018/24.09.2007, 2007.
[13] M.D. Staicovici, Coabsorbent technology for heat pumping and power production applications. Incorporate Power-Absorption Engineering (IPAE) prospectus, 2007.
[14] M.D. Staicovici, Coabsorbent cycles. Part II: Applications, in preparation, 2007.
[15] M.D. Staicovici, Coabsorbent heat pumps, accepted for presentation to the 9th IEA Heat Pumps Conference, Zurich, May 2008.
[16] M.D. Staicovici, Proposals for the Nine Sigma RPF 11087-1: Highly Efficient Low Temperature Heat Driven Cooling Technologies, March 2008.
[17] W. Niebergall, Handbuch der Kältetechnik, Band 7, Sorptions-Kältemaschinen, Springer-Verlag, Berlin, 1959.
[18] H. Perez Blanco, Conceptual design of high-efficiency absorption cooling cycle, Int. J. Refrigeration 16 (6) (1993) 429–433.
[19] H.D. Baehr, The COP of absorption and resorption heat pumps with ammonia–water as working fluids, Int. J. Refrigeration 4 (2) (1981) 83–86.
[20] T. Kashiwagi, Advances in working fluids and cycles for absorption systems, Private communication, Tokyo University of Agriculture & Technology, 1980–1990.
[21] M.D. Staicovici, Researches concerning complex absorption refrigerating machines, in: Proc. 2nd Nat. Energy Conf., 1992, pp. 89–95.
[22] F. Ziegler, et al., Multi-effect absorption chillers, Int. J. Refrigeration 16 (5) (1993) 301–311.